HOKKAIDO UNIVERSITY

Title	Azo-Crosslinked Double-Network Hydrogels Enabling Highly Efficient Mechanoradical Generation
Author(s)	Wang, Zhi Jian; Jiang, Julong; Mu, Qifeng; Maeda, Satoshi; Nakajima, Tasuku; Gong, Jian Ping
Citation	Journal of the American Chemical Society, 144(7), 3154-3161 https://doi.org/10.1021/jacs.1c12539
Issue Date	2022-02-23
Doc URL	http://hdl.handle.net/2115/88166
Rights	This document is the Accepted Manuscript version of a Published Work that appeared in final form in Journal of the American Chemical Society, copyright c American Chemical Society after peer review and technical editing by the publisher. To access the final edited and published work see https://pubs.acs.org/articlesonrequest/AOR-JDSCFNCTUZJX4EJZAUQE.
Type	article (author version)
Additional Information	There are other files related to this item in HUSCAP. Check the above URL.
File Information	J. Am. Chem. Soc._144(7)_3154-3161.pdf

Azo-crosslinked double network hydrogels enabling highly efficient mechanoradical generation

Zhi Jian Wang,[1] Julong Jiang,[2] Qifeng Mu,[1] Satoshi Maeda,[2,3,*] Tasuku Nakajima,[3,4,*] Jian Ping Gong[3,4,*]

[1]Graduate School of Life Science, Hokkaido University, Sapporo 001-0021, Japan.

[2]Department of Chemistry, Faculty of Science, Hokkaido University, Sapporo 060-8628, Japan.

[3]Institute for Chemical Reaction Design and Discovery (WPI-ICReDD), Hokkaido University, Sapporo 001-0021, Japan.

[4]Faculty of Advanced Life Science, Hokkaido University, Sapporo 001-0021, Japan.

ABSTRACT: Double network (DN) hydrogels have recently been demonstrated to generate numerous radicals by the homolytic bond scission of the brittle first network under the influence of an external force. The mechanoradicals thus generated can be utilized to trigger polymerization inside the gels, resulting in significant mechanical and functional improvements to the material. Although the concentration of mechanoradicals in DN gels is much higher than that in single network hydrogels, a further increase in the mechanoradical concentration in DN gels will widen their application. In the present work, we incorporate an azoalkane crosslinker into the first network of DN gels. Compared with the traditional crosslinker *N, N'*-methylenebis(acrylamide), the azoalkane crosslinker causes a decrease in the yield stress but significantly increases the mechanoradical concentration of DN gels after stretching. In the azoalkane-crosslinked DN gels, the concentration of mechanoradicals can reach a maximum of ~220 μM, which is five times that of the traditional crosslinker. In addition, DN gels with azoalkane crosslinker show a much higher energy efficiency for mechanoradical generation. Interestingly, DN gels crosslinked by a mixture of azoalkane crosslinker and traditional crosslinker also exhibit excellent radical generation performance. The increase in the mechanoradical concentration accelerates polymerization and can broaden the application range of force-response DN gels to biomedical devices and soft robots.

1. Introduction

Living things are open and dynamic "growing" materials, the structures of which are constantly upgraded via restructuring using building blocks such as amino acids acquired from their environment. While most artificial materials can be considered close and static, and do not exhibit such natural growth, we recently designed self-growing double network (DN) hydrogels induced by mechanical training.[1] DN hydrogels have received increasing attention as promising soft and tough hydrogels owing to their unique mechanism to offer materials with excellent mechanical strength and toughness.[2-5] DN gels consist of two interpenetrating polymer networks with contrasting mechanical properties. As a typical example, one is highly crosslinked brittle poly(2-acrylamido-2-methyl-1-propanesulfonic acid) (PAMPS) as the first network, the other is loosely crosslinked stretchable polyacrylamide (PAAm) as the second network. Such contrasting structure leads to a great number of bond ruptures of the first network to help dissipate energy during loading, whereas the second network maintains the integrity of the gel. This massive cleavage of the first network strands accompanies the generation of chemically active (mechano)radicals inside the DN gels.[1,6] Moreover, as the semi-open system of the gel allows the exchange of molecules through its interface, a DN gel immersed in a monomer solution can uptake monomer units through diffusion. Thus, when such a monomer-enriched DN gel is deformed, a large amount of mechanoradicals is generated through the

rupture of the first network strands, which in turn triggers the polymerization of monomers present within the DN gels. The destruction of the original first network and construction of new polymers leads to the "growth" of the DN gels; *i.e.* mass increase, repeated strengthening, and addition of functionalities originating from the newly synthesized polymer. Such self-growing hydrogels should find use in the biomedical devices and soft robots that require the adaptive mechanical and biochemical properties under the external force.[7,8]

The first network of the DN gels used in the previous work is composed of the main chains of carbon-carbon bonds and the cross-linking points containing amide bonds. The concentration of mechanoradicals in such DN gels after deformation was found to be approximately 10 μM.[1] Although it is much higher than that in the conventional single network hydrogels[9] and thus able to induce radical polymerization, a further increase in the concentration of mechanoradicals will provide added benefits, such as a relaxation in the requirements for an anaerobic environment for polymerization and an increase in the reaction rate, thereby widening the application fields of self-growing DN gels.

Incorporating weak covalent bonds in polymer materials is a practical strategy for designing mechanosensitive materials based on mechanochemistry. Weak covalent bonds have a lower bond dissociation energy (BDE) than strong bonds (e.g., C-C, C-N, and C-O; BDE ~ 250-400 kJ/mol)

which exist widely in the polymer chain.[10-11] Thus, when embedded in polymeric materials, they can undergo site-specific bond scissions or chemical transformations in response to mechanical forces. These weak bonds include scissile bonds that break into two parts such as the peroxide bond,[12,13] disulfide group,[14,15] and azoalkane group,[16,17] and non-scissile bonds that just change their conformation and still retain their integrity, such as the azobenzene group[18,19] and spirogyra group.[20-25] Researchers have introduced suitable weak covalent bonds into the polymer backbone to realize the required mechanoresponsive functions.[12-25]

Among these weak bonds, we focused on azoalkane (R-N=N-R; BDE ∼ 80-160 kJ/mol), whose azo group is connected to saturated carbon atoms, as an efficient mechanoradical source. Azoalkane is one of the most widely used weak covalent bonds as the initiators for radical polymerization. Azoalkane undergoes homolysis cleavage and forms reactive radicals to trigger the polymerization when exposed to heat and light.[26] In addition, azoalkane also exhibits site-specific bond cleavage when subjected to mechanical forces.[16,17] Hence, in an attempt to increase the mechanoradical concentration of DN gels under a mechanical force, an azoalkane crosslinker is adopted for the first PAMPS network. Owing to the low BDE of azoalkane, improvement of energy efficiency for radical generation in the deformed DN gel is expected.

In order to investigate the effect of the azoalkane crosslinker on the mechanical properties of the gel and bond rupture process during loading, three types of DN gels are synthesized following the conventional two-step sequential polymerization process, as shown in Fig. 1a: A traditional DN-MBA gel, in which the first PAMPS network is crosslinked by the conventional crosslinker *N,N'*-methylenebis(acrylamide) (MBA) (Fig. 1a$_4$ and 1b); a DN-AAC gel, in which the first PAMPS network is crosslinked by an azoalkane crosslinker (AAC) (Fig. 1a$_5$ and 1c, see SI Fig. S1); and a DN-MIX gel, in which a 1:1 molar ratio mixture of MBA and AAC crosslinks the first PAMPS network (Fig. 1a$_6$). Since azoalkane group is also sensitive to high temperature and UV light, the radical polymerizations of the first and second networks were performed at 44°C for 10 h with the low temperature thermal initiator to avoid decomposition of the azoalkane group in AAC during the hydrogel preparation. Thermal decomposition of the AAC during the polymerizations was found to be negligible (see SI Fig. S2).
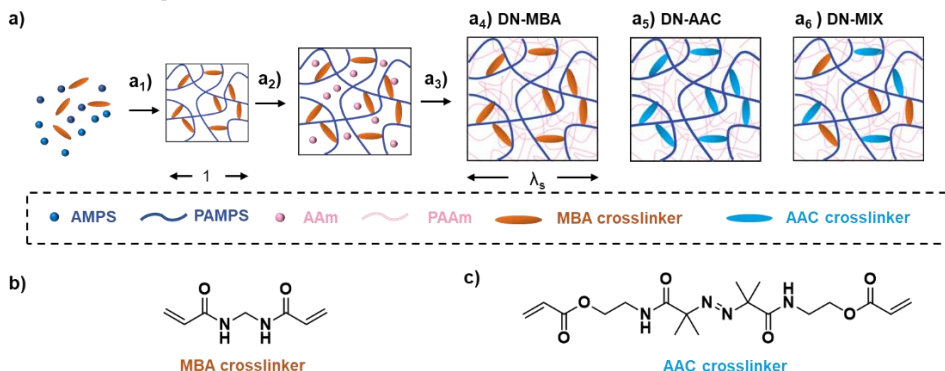
Figure 1. Preparation of DN gels with different crosslinkers. (a) By two step sequential polymerization (a$_1$-a$_3$) and varying the crosslinker in the first step of polymerization (a$_1$), DN gels with different crosslinkers (a$_4$-a$_6$) are synthesized: (a$_1$) synthesizing PAMPS SN gels, (a$_2$) immersing PAMPS SN gels in an acrylamide (AAm) solution, (a$_3$) synthesizing the second AAm network in PAMPS gels and then immersing them into pure water to obtain equilibrated DN gels (a$_4$-a$_6$). The length swelling ratio λ_s of the PAMPS network in DN gels is determined by the thickness of the equilibrated DN gels (a$_4$-a$_6$) divided by the thickness of the as-prepared PAMPS SN gels. (b-c) Chemical structure of MBA (b) and AAC (c) crosslinkers.

2. Results and Discussion

2.1 Density functional theory simulation of the bond rupture under the force

To understand how the external force promotes the rupture of PAMPS network, we first construct a PAMPS network fragment that consists of four AMPS units (-CH$_2$SO$_3$Na group is simplified to -CH$_3$ to reduce computational cost) and one AAC or one MBA unit (Fig. 2a and 2b) for our theoretical study. The simulation of the tensile force used to break the covalent bond is realized by our Artificial Force Induced Reaction (AFIR) method.[27,28] The AFIR method explicitly adds an artificial force between the certain fragments of a molecule to trigger a reaction. The force is applied to the system by the following AFIR function:
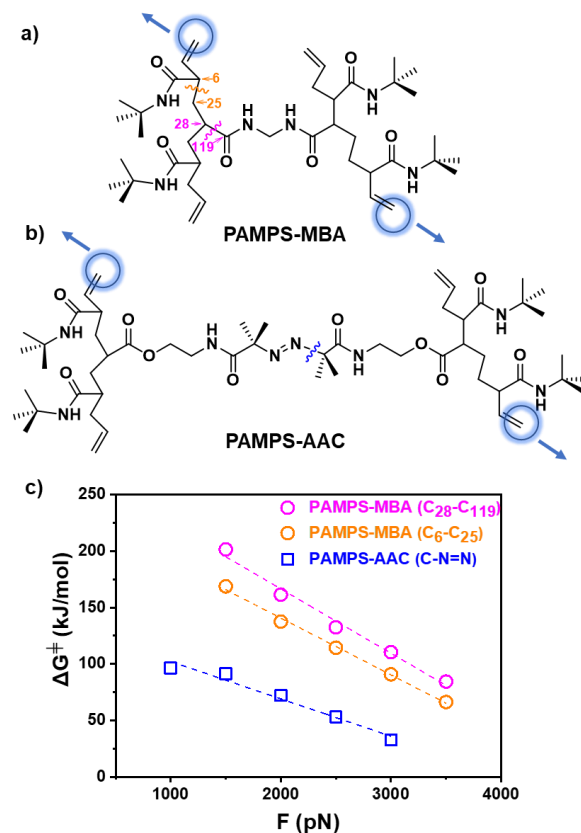
$$F^{AFIR}(\mathbf{Q}) = E(\mathbf{Q}) + \rho\alpha\frac{\sum_{i\in A}\sum_{j\in B}\omega_{ij}r_{ij}}{\sum_{i\in A}\sum_{j\in B}\omega_{ij}} \qquad (1)$$

In Eq. (1), $E(\mathbf{Q})$ is the original Born-Oppenheimer potential energy surface of the given geometrical parameter $\mathbf{Q}$ and the second term applies the force to the system of interest. The parameter α, controls the strength of the force added to the designated fragments inside the molecule of interest. The force term is given as a weighted sum of the distances r_{ij} between atom i in the fragment A and atom j in the fragment B through weight function ω_{ij} (see SI). Normally, an artificial attractive force (i.e., ρ = +1 in Eq. (1)) is applied to suppress the potentially reactive atoms into a certain short distance so that a reaction can proceed. In this case, a repulsive force (realized by setting ρ to -1) is added to the two terminal CH$_2$ groups of the polymer fragment. Such a repulsive force therefore acts as an external tensile force that stretches the polymer chain, which models what a

polymer chain experiences in the single-molecule force spectroscopy experiment. With this diagonally-added artificial force, both the PAMPS chain and the MBA molecule can experience the same level of force at the same time, therefore allowing us to explore all the possible cleavage sites in the polymer network. The above-mentioned AFIR function can be used to construct the force modified potential energy surface (FMPES). Our efforts were subsequently made to locate the transition state (TS) of the bond homolysis process for both PAMPS-MBA and PAMPS-AAC networks on such an FMPES. Once the TS structure on the FMPES is successfully optimized, the Gibbs energy barrier for the formation of mechanoradicals under that certain level of force can be realized. With the varying force level (F), we can eventually characterize how the Gibbs energy barrier ($\Delta G^{\ddagger}$) changes accordingly. With this $\Delta G^{\ddagger}$-F relationship acquired from TS optimization, the rupture force can be determined at a given time. As shown in Fig. 2a and 2b, based on our calculations, there are two possible rupture sites in PAMPS-MBA network, either at C_6-C_{25} or C_{28}-C_{119} position (see SI Fig. S3), while there is only one rupture site at the C-(N=N) position for PAMPS-AAC network (see SI Fig. S4). Our TS calculations revealed that the Gibbs energy barrier for the rupture of PAMPS-MBA at C_6-C_{25} site or C_{28}-C_{119} site is much higher than that of PAMPS-AAC network at C-(N=N) position. Given a certain timescale (*e.g.*, 11.6 s ~ 1.44 min, which corresponds to a barrier of 80 ~ 85 kJ/mol under room temperature according to the Eyring equation), the rupture force of PAMPS-MBA network is 3110 ~ 3210 pN at C_6-C_{25} position while that of the PAMPS-AAC network is only 1520 ~ 1670 pN (Fig. 2c). These calculation results strongly suggest that a large number of mechanoradicals can be effectively generated through PAMPS-AAC network.

Figure 2. DFT simulation of the bond rupture under an external force. (a,b) Model molecule as the PAMPS-MBA (a) and PAMPS-AAC (b) network employed in the DFT calculations. Blue circle regions represent the fragments (i.e., CH_2 groups) of the molecule where artificial forces are added diagonally. (c) Relationship between the Gibbs energy barriers ($\Delta G^{\ddagger}$) of the covalent bond homolysis and the level of artificial tensile force (F).

## 2.2 Influence of azoalkane group on the mechanical properties

We first compare the structure of the PAMPS single network (SN) hydrogels formed by different crosslinkers from their modulus and swelling ability. We vary the crosslinker concentration in feed during the first step of the polymerization of AMPS (C_{1st}, mol% in relative to AMPS monomer), whereas the second network is prepared using the same formulation for all three sets of DN gels. Fig. 3a shows the Young's modulus of the as-prepared PAMPS SN gels ($E_{as\text{-}prep,1st}$) obtained using different crosslinkers. According to the phantom network model for a network with four-branched crosslinking points,[29] the number density of elastically effective polymer strands of the as-prepared PAMPS network (ν_{1st}) is proportional to its Young's modulus through the relation $\nu_{1st} = 2E_{as\text{-}prep,1st} / 3RT$, where R and T are the gas constant and absolute temperature, respectively. At the same C_{1st}, PAMPS SN gels crosslinked by AAC have a smaller Young's modulus than those crosslinked by MBA, indicating a lower ν_{1st} of the PAMPS SN gel when crosslinked by AAC. The PAMPS-MIX SN gels have almost the same $E_{as\text{-}prep,1st}$ with PAMPS-AAC at the same C_{1st}, indicating the same

crosslinking density of these two sets of gels. Nevertheless, the PAMPS-AAC SN gels show larger swelling than PAMPS-MIX when immersed in the AAm monomer solution (see SI Fig. S5), leading to a higher length swelling ratio (λ_s) of the PAMPS-AAC network in the final equilibrated state compared with that of DN-MIX (Fig. 3b). This indicates that the MBA crosslinker has a less swelling ability in water than AAC. Accordingly, the lower λ_s of DN-MBA, as depicted in Fig. 3b, should be attributed to the higher crosslinking density of the MBA crosslinker and the lower swelling ability.

The mechanical performance of DN gels with different first network crosslinker varieties and concentrations is investigated using uniaxial tensile tests. As shown in Fig. 3c-e, three sets of DN gels show the same trend—the yield stress (σ_y, Fig. 3g), modulus (E, see SI Fig. S6a), and fracture stress (σ_f, see SI Fig. S6b) increase substantially with an increase in C_{1st}. On the other hand, the yield strain (ε_y, Fig. 3f) depends weakly on C_{1st}, and the fracture strain (ε_f, see SI Fig. S6c) tends to decrease with an increase in C_{1st}. This dependence on the crosslinker concentration is consistent with our previous work.[30,31]
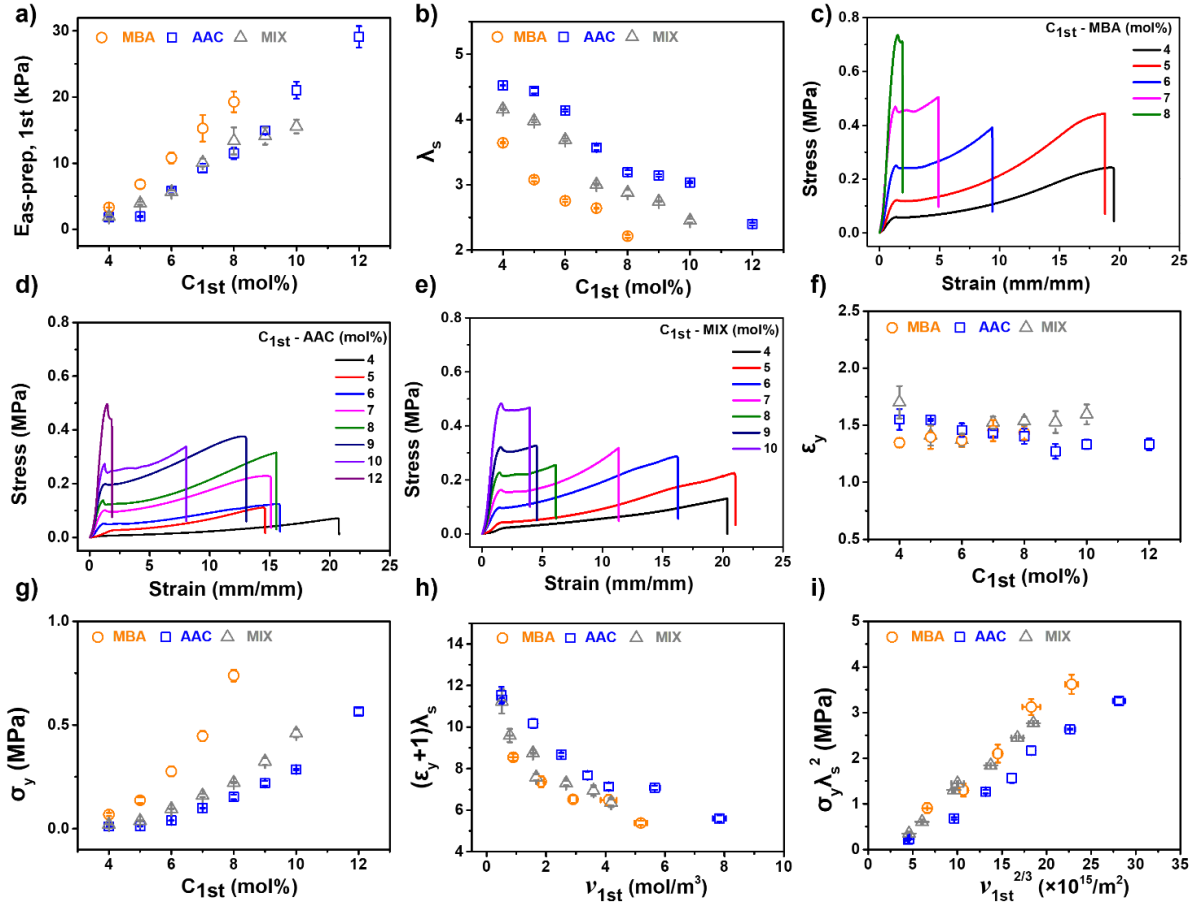
Figure 3. Dependence of mechanical properties on the crosslinker species. (a) Young's modulus of as-prepared PAMPS SN gels $E_{as-prep,1st}$ with respect to the crosslinker concentration C_{1st}. (b) Length swelling ratio (λ_s) of the PAMPS network in DN gels with C_{1st}. (c-g) Tensile stress-strain curves of DN-MBA (c), DN-AAC (d), and DN-MIX (e) and corresponding yield strain ε_y (f) and yield stress σ_y (g) with C_{1st}. (h) Rescaled yield strain $(\varepsilon_y+1)\lambda_s$ with the effective crosslinking density of the PAMPS SN hydrogels ν_{1st}. (i) Rescaled yield stress $(\sigma_y\lambda_s^2)$ with the effective area crosslinking density of the PAMPS SN hydrogels $\nu_{1st}^{2/3}$. The error bars represent the standard deviations among at least three measurements.

In order to compare the effect of crosslinkers on the internal fracture of the first network, we first discuss the yield point of these DN gels since yield point is characteristic to the stretching limit of the first network.[32] In all three sets of samples, yielding is observed at strains between 1.3 and 1.6. ε_y at the same C_{1st} shows less dependence on the crosslinker species. In contrast, σ_y is strongly affected by the crosslinker species. For the DN-MBA gels, σ_y increases from 0.07 MPa to 0.74 MPa when C_{1st} is increased from 4 mol% to 8 mol%, which is much higher than σ_y of DN-AAC gels (0.01 MPa - 0.15 MPa) at the same C_{1st}. Even when the C_{1st} of AAC is increased to 12 mol%, at which the DN-AAC gel breaks just after reaching the yield point, σ_y is only 0.57 MPa, still much lower than the σ_y of the DN-MBA gel with a C_{1st} of 8 mol%.

To further quantitatively study the influence of the weak azoalkane group in the PAMPS network, we need to normalize the network density and prestretch level of the PAMPS network in the three systems. We take the as-prepared PAMPS single network (SN) gels as the reference state. Based on the swelling ratio in length, we can obtain the normalized yield stress ($\sigma_y\lambda_s^2$) and yield stretch ratio ($(\varepsilon_y+1)\lambda_s$) to their respective reference states for the three sets of DN

gels. Fig. 3h shows the normalized yield stretch ratio $(\varepsilon_y+1)\lambda_s$ replotted as a function of ν_{1st}. At the same ν_{1st}, especially at a low ν_{1st}, the $(\varepsilon_y+1)\lambda_s$ of the DN-AAC gels is larger than that of the DN-MBA gels, indicating the better stretchability of the PAMPS network when crosslinked by AAC. For normalized yield stress $\sigma_y\lambda_s^2$, it should be proportional to the area density ($\nu_{1st}^{2/3}$) of the PAMPS network strands at the reference state times bond breaking force per strand (F)[31]:

$$\sigma_y\lambda_s^2 \propto \nu_{1st}^{2/3} \times F \quad (2)$$

As shown in Fig. 3i, the $\sigma_y\lambda_s^2$ of the three sets of DN gels increase almost linearly with $\nu_{1st}^{2/3}$, confirming the relationship of (2). The slope of the linear regression line of DN-AAC is approximately 30% smaller than that of DN-MBA. This result is reasonably in consistent with DFT calculation, clearly demonstrating that the bond breaking force of the PAMPS network crosslinked by AAC is lower than that of the network crosslinked by MBA. As for the DN-MIX gels, they show the mechanical properties closer to DN-MBA.

2.3 Influence of azoalkane group on the mechanoradical concentration

Next, we investigate the mechanoradical concentration (C_{rad}) of the DN gels generated on stretching, by applying Fenton color reactions.[1,33,34] The preset strain is chosen at $\varepsilon_{max} = 4$, which is well beyond the yield point but still not reaching the strain-hardening region, thereby bond rupture of the second network is considered negligible. A discussion on brittle DN gels with a high C_{1st} is not included here, as they break immediately after reaching the yield point. DN gels fed with ferrous ions (Fe^{2+}) and xylenol orange (XO) are loaded to the preset strain in air (Fig. 4a$_1$ and 4a$_2$) and then unloaded immediately. During the process, the stress-strain curves for loading and unloading are recorded, and the hysteresis area between the loading and unloading curves is calculated to estimate the dissipated energy (U_{hys}, Fig. 4a$_4$). The ferric ion (Fe^{3+}) concentration in the necked regions of the samples is reflected on the color change due to the complex formation of XO-Fe^{3+} and can be detected through an ultraviolet-visible light spectrum (see SI Fig. S7). Assuming that all types of mechanoradicals generated by bond scission have the same reactivity in the Fenton solution, C_{rad} can be considered equal to the Fe^{3+} concentration.
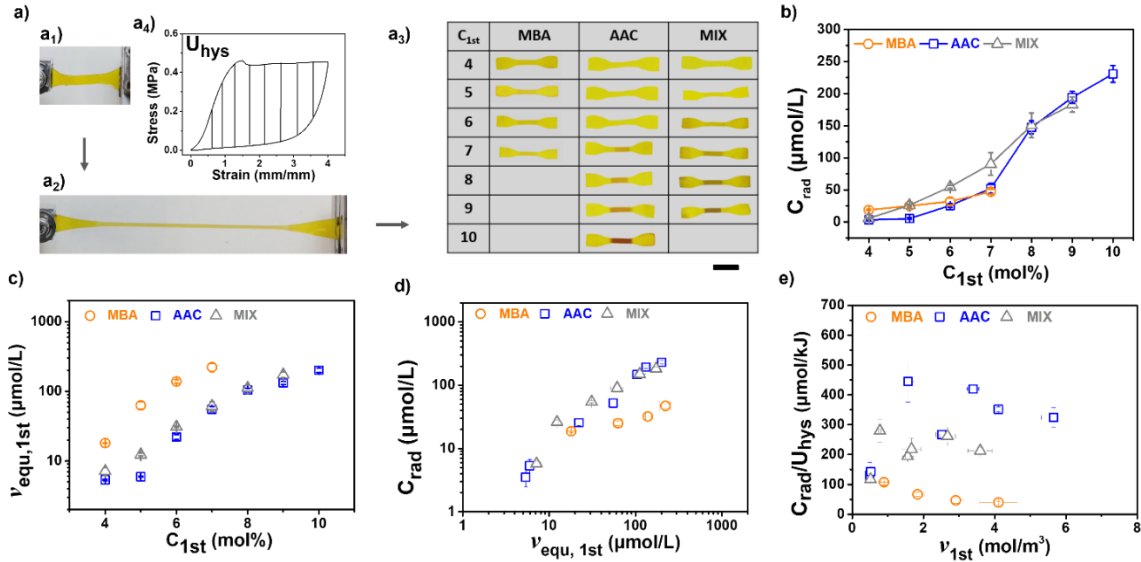
Figure 4. Characterization of mechanoradicals in DN gels after stretching by the Fenton color reaction. (a) Photographic images of DN gels fed with Fe^{2+} and XO before (a$_1$), during (a$_2$), and 30 min after stretching (a$_3$). Scale bar: 2 cm. The inset (a$_4$) is the representative stress-strain curve recorded during loading and unloading, and the area between the loading and unloading curves is the dissipated energy U_{hys}. (b) Mechanoradical concentration C_{rad} as a function of C_{1st}. (c) The PAMPS network density at swelling equilibrated state ($\nu_{equ,1st}$) as a function of C_{1st}. (d) C_{rad} as a function of $\nu_{equ,1st}$. (e) Energy efficiency for radical generation C_{rad}/U_{hys} as a function of the effective crosslinking density of the PAMPS SN hydrogels ν_{1st}. The error bars represent the standard deviations among at least three measurements.

The results are shown in Fig. 4a$_3$ and 4b. All three types of DN gels show an increase in C_{rad} with an increase in C_{1st}. As the DN-MBA gels become brittle at C_{1st} above 7 mol% while DN-AAC gels show necking until 10 mol%, the DN gel crosslinked with 10 mol% AAC exhibits the highest C_{rad} of ~220 μM among all DN gels, which is five times the highest C_{rad} generated by the DN-MBA system. Thus, our initial aim to generate a higher concentration of mechanoradicals is realized by introducing AAC crosslinks. Interestingly, the dominant species to generate radicals are not always DN-AAC gels. At the C_{1st} values of 6 mol% and 7 mol%, the DN-MIX gels are capable of generating more radicals than the other two sets of DN gels. And at C_{1st} values of 8 mol% and 9 mol%, the C_{rad} of DN-MIX is almost equal to that of the DN-AAC gels. These results show that the use of a mixture of MBA and AAC crosslinkers in the synthesis of DN gels can also generate a high C_{rad}, which is beneficial for reducing the amount of AAC used.

As analyzed previously, the mechanoradicals are generated from the bond rupture of the first network strands. Thus, the C_{rad} is proportional to the PAMPS network density at swelling equilibrated state ($\nu_{equ,1st} = \nu_{1st} / \lambda_s^3$) at which the mechanical deformation was performed. As shown in Fig. 4c, $\nu_{equ,1st}$ increases with C_{1st} for all three DN gels and $\nu_{equ,1st}$ of DN-MBA is larger than that of DN-AAC and DN-MBA at the same C_{1st}. As depicted in Fig. 4d, for the same $\nu_{equ,1st}$, C_{rad} of DN-AAC and DN-MIX is larger than that of DN-MBA, especially at high $\nu_{equ,1st}$. This result indicates that a larger fraction of the first network strands is ruptured when crosslinked by AAC or AAC-MBA mixture. To analyze the fraction of strand ruptured at varied crosslinking density, we express the C_{rad} as the product of the PAMPS network density ($\nu_{equ,1st}$) and the ratio of broken strands to total strands of the PAMPS network (φ_b):

$$C_{rad} = 2\,\nu_{equ,1st} \times \varphi_b \quad (3)$$

The prefactor 2 in Equation (3) is because one bond cleavage generates two radicals. The φ_b estimated from Equation (3) exhibited very different behaviors against C_{1st} and $\nu_{equ,1st}$ for the three sets of DN gels (see SI Fig. S8a and S8b). φ_b of DN-MBA monotonously decreases with increase of C_{1st} and $\nu_{equ,1st}$, whereas φ_b of DN-AAC and DN-MIX shows maximum at certain C_{1st} and $\nu_{equ,1st}$. More importantly, DN-AAC and DN-MIX show much larger φ_b than that of DN-MBA

when the C_{1st} or $\nu_{equ,1st}$ is not too low, resulting from the labile azoalkane group under the external force. The trend of φ_b gives an insight of the rupture efficiency of these DN gels. To achieve a high concentration of mechanoradicals in the stretched gels, high values for $\nu_{equ,1st}$ and φ_b are both required. The lower $\nu_{equ,1st}$ of DN-AAC at C_{1st} from 4 mol% to 7 mol% results in a lower C_{rad} than DN-MBA or DN-MIX at the same C_{1st}.

Next, we investigate the energy efficiency for radical generation in the three sets of DN gels, characterized by the ratio of C_{rad} to the dissipated energy U_{hys}. Assuming that U_{hys} is entirely consumed in the bond scissions of the first network strands, the following relation between C_{rad} and U_{hys} is obtained by applying the classical Lake-Thomas theory:[5,35]

$$C_{rad} \propto 2\, U_{hys}\, /\, NU_b \quad (4)$$

where U_b represents the dissociation energy of a single bond, and N is the monomer segment number of a strand between crosslinking points. Because the monomer concentration of the first network at preparation is the same, N is inversely proportional to ν_{1st}, assuming that all monomers are incorporated into the elastically effective strands of the network. Thus, the relation (4) can be rewritten as:

$$C_{rad}\, /\, U_{hys} \propto 2\, /\, NU_b \propto 2\, \nu_{1st}\, /\, U_b \quad (5)$$

Equation (5) predicts a higher energy efficiency for radical generation in DN-AAC gels than DN-MBA gels, as the U_b of AAC bond is much lower. As shown in Fig. 4e, at the same ν_{1st}, the C_{rad}/U_{hys} of DN-AAC is approximately ten times that of DN-MBA. This is much higher than that predicted from their difference in U_b by Equation (5). The C_{rad}/U_{hys} of DN-MIX is between those of DN-AAC and DN-MBA but much closer to that of DN-AAC gels, demonstrating that the bond scissions in the DN-MIX gel are dominated by the weak azoalkane group. These analyses confirm the feasibility of our strategy to increase the mechanoradical concentration by incorporating a weak azoalkane group into the system.

The substantially high mechanoradical concentration attained in DN gels still cannot completely eliminate the limitation of an oxygen-free environment; however, the limit to the maximum allowable dissolved oxygen in water for mechanoradical polymerization is increased, and the mechanoradical polymerization process is accelerated. To demonstrate this effect, we choose a DN-10AAC gel and a DN-7MBA gel that have the similar mechanical behaviors in their virgin state for comparison. Here the numbers 10 in 10AAC and 7 in 7MBA represent the corresponding C_{1st} values. First, we compare the force-responsive performances of two DN gels by their appearance change. After 2 h of deaeration in an argon glove box, the two DN gels fed with *N*-isopropylacrylamide (NIPAM, 2.0 M) and the MBA crosslinker (0.15 M) are compressed by a stamp with a raised bear toe shape (Fig. 5a). After 3 min, the DN-10AAC gel directly show a distinct bear toe pattern at the ambient temperature, resulting from the formation of a highly crosslinked PNIPAm network in the compressed region (Fig. 5b). This is further confirmed by the fact that the polymer weight fraction in the compressed region increases from 12% to 19% (see SI Fig. S9a). In comparison, the DN-7MBA gel shows no distinct change in appearance even after 30 min

and no increase in the polymer weight fraction, indicating that polymerization hardly occurs under the same deaeration conditions. Then we demonstrate that substantially high concentration of mechanoradicals in DN-AAC can also be used to realize a fast stretching-triggered mechanical growth of the gels. These two DN gels are fed with monomer AMPS (0.6 M) and crosslinker *N,N',N''*-triacryloyl diethylenetriamine (TADETA; 0.3 M) and are performed with cyclic loading-unloading tests twice with an interval of 3 min (Fig. 5c) in the argon glove box. In contrast to the DN-7MBA gel, which shows mechanical hysteresis only in the first cycle, the DN-10AAC gel shows hysteresis and the force increase in the second cycle (Fig. 5d). Specifically, to the same gauge length of 50 mm, the retraction force of DN-10AAC is 0.8 N at the first loading but decreases to 0.2 N at the first unloading due to the permanent rupture of the brittle network. However, at the second loading it increases to the larger value of 1.0 N. The force enhancement indicates the rapid formation of a new network in the DN-10AAC gel after the first stretching cycle due to highly efficient mechanoradical generation. In fact, the polymer weight fraction in the stretched region of DN-10AAC increases from 12% to 23%, but not in the DN-7MBA gel (see SI Fig. S9b).
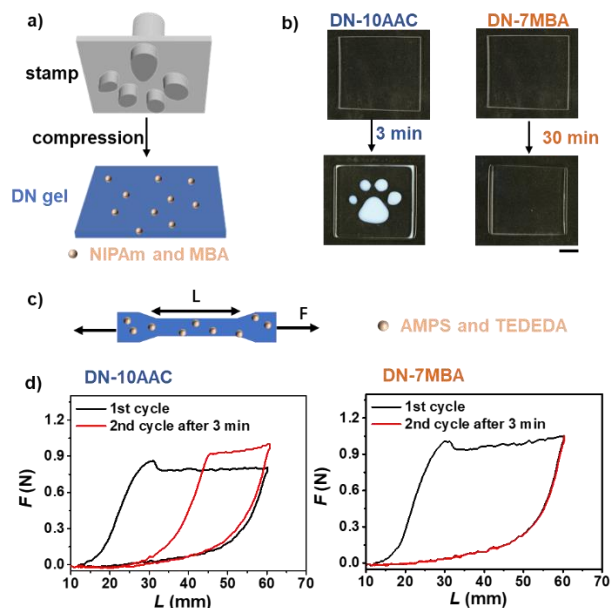
Figure 5. Fast force-responsive pattern (a,b) and strength enhancement (c,d) of DN gels with high mechanoradical concentration. (a) Illustration of DN gels fed with the monomer NIPAm and crosslinker MBA compressed by a stamp with a raised bear toe pattern. (b) Photographs of DN gels before and after compression. Scale bar: 1 cm. (c) Illustration of stretching DN gel with the supply of monomer AMPS and crosslinker TADETA. (d) Force-length curves showing the cyclic loading-unloading behavior of different DN gels. Black line: first cycle. Red line: second cycle.

3. Conclusions

In summary, we have incorporated the azoalkane crosslinker AAC into the first PAMPS network in DN gels and demonstrate that the incorporation of AAC remarkably increases the mechanoradical concentration compared to the commercial crosslinker MBA. The energy efficiency for

mechanoradical generation is also much improved by using AAC crosslinker. Employing a mixture of MBA and AAC crosslinkers results in a comparable crosslinking efficiency as MBA alone but an excellent performance in generating mechanoradicals as like AAC alone. The increased mechanoradical concentration accelerates force-triggered polymerization, which is beneficial for extending the application of DN gels in force-responsive fields.

ASSOCIATED CONTENT

Supporting information. Details of the computational simulation, reagents used, synthesis procedure and characterization of the azoalkane crosslinker, hydrogel preparation, measurement of hydrogel mechanical properties and mechanoradical concentration, methods to show fast force responsive polymerization.

AUTHOR INFORMATION

Corresponding Author

*smaeda@eis.hokudai.ac.jp; tasuku@sci.hokudai.ac.jp; gong@sci.hokudai.ac.jp

REFERENCES

1. Matsuda, T.; Kawakami, R.; Namba, R.; Nakajima, T.; Gong, J. P. Mechanoresponsive Self-Growing Hydrogels Inspired by Muscle Training. *Science* **2019**, *363* (6426), 504–508.

2. Gong, J. P.; Katsuyama, Y.; Kurokawa, T.; Osada, Y. Double Network Hydrogels With Extremely High Mechanical Strength. *Adv. Mater.* **2003**, *15* (14), 1155–1158.

3. Gong, J. P. Why Are Double Network Hydrogels so Tough? *Soft Matter* **2010**, *6* (12), 2583–2590.

4. Na, Y. H.; Tanaka, Y.; Kawauchi, Y.; Furukawa, H.; Sumiyoshi, T.; Gong, J. P.; Osada, Y. Necking Phenomenon of Double-Network Gels. *Macromolecules* **2006**, *39* (14), 4641–4645.

5. Nakajima, T.; Kurokawa, T.; Ahmed, S.; Wu, W. L.; Gong, J. P. Characterization of Internal Fracture Process of Double Network Hydrogels Under Uniaxial Elongation. *Soft Matter* **2013**, *9* (6), 1955–1966.

6. Matsuda, T.; Kawakami, R.; Nakajima, T.; Gong, J. P. Crack Tip Field of a Double-Network Gel: Visualization of Covalent Bond Scission Through Mechanoradical Polymerization. *Macromolecules* **2020**, *53* (20), 8787–8795.

7. Nonoyama, T.; Gong, J. P. Tough Double Network Hydrogel and Its Biomedical Applications. *Annu. Rev. Chem. Biomol. Eng.* **2021**, 12, 1-18.

8. Liu, X. Y.; Liu, J.; Lin, S. T.; Zhao, X. H. Hydrogel Machines. *Mater. Today* **2020,** 36, 102-124.

9. Fitch, K. R.; Goodwin, A. P. Mechanochemical Reaction Cascade for Sensitive Detection of Covalent Bond Breakage in Hydrogels. *Chem. Mater.* **2014**, *26* (23), 6771–6776.

10. Zavitsas, A. A. The Relation Between Bond Lengths and Dissociation Energies of Carbon–Carbon Bonds. *J. Phys. Chem. A* **2003**, *107* (6), 897–898.

11. Li, J.; Nagamani, C.; Moore, J. S. Polymer Mechanochemistry: From Destructive to Productive. *Acc. Chem. Res.* **2015**, *48* (8), 2181–2190.

12. Encina, M. V.; Lissi, E.; Sarasúa, M.; Gargallo, L.; Radic, D. Ultrasonic Degradation of Polyvinylpyrrolidone: Effect of Peroxide Linkages. *J. Polym. Sci. Polym. Lett. Ed.* **1980**, *18* (12), 757–760.

13. Chen, Y. L.; Spiering, A. J. H.; Karthikeyan, S.; Peters, G. W. M.; Meijer, E. W. R.; Sijbesma, R. P. Mechanically Induced Chemiluminescence From Polymers Incorporating a 1,2-Dioxetane Unit in the Main Chain. *Nat. Chem.* **2012**, *4* (7), 559–562.

14. Li, Y. C.; Nese, A.; Matyjaszewski, K.; Sheiko, S. S. Molecular Tensile Machines: Anti-Arrhenius Cleavage of Disulfide Bonds. *Macromolecules* **2013**, *46* (18), 7196–7201.

15. Lee, J.; Silberstein, M. N.; Abdeen, A. A.; Kim, S. Y.; Kilian, K. A. Mechanochemical Functionalization of Disulfide Linked Hydrogels. *Mater. Horiz.* **2016**, *3* (5), 447–451.

16. Berkowski, K. L.; Potisek, S. L.; Hickenboth, C. R.; Moore, J. S. Ultrasound-Induced Site-Specific Cleavage of Azo-Functionalized Poly(Ethylene Glycol). *Macromolecules* **2005**, *38* (22), 8975–8978.

17. Lee, B.; Niu, Z. B.; Wang, J. P.; Slebodnick, C.; Craig, S. L. Relative Mechanical Strengths of Weak Bonds in Sonochemical Polymer Mechanochemistry. *J. Am. Chem. Soc.* **2015**, *137* (33), 10826–10832.

18. Surampudi, S. K.; Patel, H. R.; Nagarjuna, G.; Venkataraman, D. Mechano-Isomerization of Azobenzene. *Chem. Commun.* **2013**, *49* (68), 7519–7521.

19. Lin, Y. J.; Hansen, H. R.; Brittain, W. J.; Craig, S. L. Strain-Dependent Kinetics in the Cis-to-Trans Isomerization of Azobenzene in Bulk Elastomers. *J. Phys. Chem. B* **2019**, *123* (40), 8492–8498.

20. Davis, D. A.; Hamilton, A.; Yang, J.; Cremar, L. D.; Gough, D. V.; Potisek, S. L.; Ong, M. T.; Braun, P. V.; Martinez, T. J.; White, S. R.; Moore, J. S.; Sottos, N. R. Force-Induced Activation of Covalent Bonds in Mechanoresponsive Polymeric Materials. *Nature* **2009**, *459*, 69–72.

21. Kingsbury, C. M.; May, P. A.; Davis, D. A.; White, S. R.; Moore, J. S.; Sottos, N. R. Shear Activation of Mechanophore-crosslinked Polymers. *J. Mater. Chem.* **2011**, *21* (23), 8381–8388.

22. Chen, Y. J.; Yeh, C. J.; Qi, Y.; Long, R.; Creton, C. From Force-Responsive Molecules to Quantifying and Mapping Stresses in Soft Materials. *Sci. Adv.* **2020**, *6* (20), eaaz5093.

23. Chen, Y. J.; Yeh, C. J.; Guo, Q.; Qi, Y.; Long, R.; Creton, C. Fast Reversible Isomerization of Merocyanine as a Tool to Quantify Stress History in Elastomers. *Chem. Sci.* **2020**, *12* (5), 1693–1701.

24. Chen, Y. J.; Sanoja, G.; Creton, C. Mechanochemistry Unveils Stress Transfer During Sacrificial Bond Fracture of Tough Multiple Network Elastomers. *Chem. Sci.* 2021, *12* (33), 11098–11108 DOI: 10.1039/d1sc03352b.

25. Qiu, W.; Gurr, P. A.; Qiao, G. G. Regulating Color Activation Energy of Mechanophore-Linked Multinetwork Elastomers. *Macromolecules* **2020**, *53* (10), 4090–4098.

26. Aubert, M.; Roth, M.; Pfaendner, R.; Wilén, C. E. Azoalkanes: a Novel Class of Additives for Cross-Linking and Controlled Degradation of Polyolefins. *Macromol. Mater. Eng.* **2007**, *292* (6), 707–714.

27. Maeda, S.; Ohno, K.; Morokuma, K. Systematic Exploration of the Mechanism of Chemical Reactions: the Global Reaction Route Mapping (GRRM) Strategy Using the ADDF and AFIR Methods. *Phys. Chem. Chem. Phys.* **2013**, *15* (11), 3683–3701.

28. Maeda, S.; Harabuchi, Y. Exploring Paths of Chemical Transformations in Molecular and Periodic Systems: an Approach Utilizing Force. *WIREs Comput. Mol. Sci.* **2021**, *11* (6), e1538.

29. Rubinstein, M.; Colby, R. *Polymer Physics*; Oxford, **2003**, pp 262–266.

30. Ahmed, S.; Nakajima, T.; Kurokawa, T.; Anamul Haque, M. A.; Gong, J. P. Brittle-Ductile Transition of Double Network Hydrogels: Mechanical Balance of Two Networks as the Key Factor. *Polymer* **2014**, *55* (3), 914‑923.

31. Nakajima, T.; Kurokawa, T.; Furukawa, H.; Gong, J. P. Effect of the Constituent Networks of Double Network Gels on Their Mechanical Properties and Energy Dissipation Process. *Soft Matter* **2020**, *16* (37), 8618–8627.

32. Matsuda, T.; Nakajima, T.; Fukuda, Y.; Hong, W.; Sakai, T.; Kurokawa, T.; Chung, U. I.; Gong, J. P. Yielding Criteria of Double Network Hydrogels. *Macromolecules* **2016,** *49* (5), 1865–1872.

33. Gay, C.; Collins, J.; Gebicki, J. M. Determination of Iron in Solutions With the Ferric-Xylenol Orange Complex. *Anal. Biochem.* **1999**, *273* (2), 143–148.

34. Baytekin, H. T.; Baytekin, B.; Grzybowski, B. A. Mechanoradicals Created in "Polymeric Sponges" Drive Reactions in Aqueous Media. *Angew. Chem. Int. Ed. Engl.* **2012**, *51* (15), 3596–3600.

35. Lake, G. J.; Thomas, A. G. The Strength of Highly Elastic Materials. *Proc. R. Soc. Lond. A* **1967**, *300* (1460), 108–119.